Author Manuscript

Author Manuscript

Author Manuscript

Author Manuscript

HHS Public Access

Author manuscript

Neuroscience. Author manuscript; available in PMC 2020 April 15.

Published in final edited form as:

Neuroscience. 2019 April 15; 404: 338–352. doi:10.1016/j.neuroscience.2019.01.066.

Impaired cognitive flexibility following NMDAR-GluN2B deletion is associated with altered orbitofrontal-striatal function

Kristin Marquardt[1], **Megan Josey**[1], **Johnny A. Kenton**[1], **James F. Cavanagh**[2], **Andrew Holmes**[3], and **Jonathan L. Brigman**[*,1,4]

[1]Department of Neurosciences, University of New Mexico School of Medicine, Albuquerque, NM

[2]Department of Psychology, University of New Mexico

[3]Laboratory of Behavioral and Genomic Neuroscience, National Institute on Alcohol Abuse and Alcoholism, Bethesda, Maryland, USA

[4]New Mexico Alcohol Research Center, UNM Health Sciences Center, Albuquerque, NM

Abstract

A common feature across neuropsychiatric disorders is inability to discontinue an action or thought once it has become detrimental. Reversal learning, a hallmark of executive control, requires plasticity within cortical, striatal and limbic circuits and is highly sensitive to disruption of *N*-methyl-$_D$-aspartate receptor (NMDAR) function. In particular, selective deletion or antagonism of GluN2B containing NMDARs in cortical regions including the orbitofrontal cortex (OFC), promotes maladaptive perseveration. It remains unknown whether GluN2B functions to maintain local cortical activity necessary for reversal learning, or if it exerts a broader influence on the integration of neural activity across cortical and subcortical systems. To address this question, we utilized *in vivo* electrophysiology to record neuronal activity and local field potentials (LFP) in the orbitofrontal cortex and dorsal striatum (dS) of mice with deletion of GluN2B in neocortical and hippocampal principal cells while they performed touchscreen reversal learning. Reversal impairment produced by corticohippocampal GluN2B deletion was paralleled by an aberrant increase in functional connectivity between the OFC and dS. These alterations in coordination were associated with alterations in local OFC and dS firing activity. These data demonstrate highly dynamic patterns of cortical and striatal activity concomitant with reversal learning, and reveal GluN2B as a molecular mechanism underpinning the timing of these processes.

Keywords

executive function; in vivo electrophysiology; NMDAR. Local field potentials

[*]Corresponding author: Jonathan L. Brigman, PhD, Department of Neurosciences, University of New Mexico School of Medicine, MSC08 4740, 1 University of New Mexico, Albuquerque, NM, USA 87131-0001, jbrigman@salud.unm.edu, Telephone: 505-272-2868, Fax: 505-272-8082.

Publisher's Disclaimer: This is a PDF file of an unedited manuscript that has been accepted for publication. As a service to our customers we are providing this early version of the manuscript. The manuscript will undergo copyediting, typesetting, and review of the resulting proof before it is published in its final citable form. Please note that during the production process errors may be discovered which could affect the content, and all legal disclaimers that apply to the journal pertain.

Author Manuscript Author Manuscript Author Manuscript Author Manuscript

Introduction

Deficient executive function has come into increasing focus as a priority area for the development of novel therapeutic treatments for multiple neuropsychiatric, developmental, and substance abuse disorders [1]. One domain of impaired executive control is maladaptive perseveration - an inability to discontinue a previously advantageous response when it is no longer beneficial [2, 3]. Reversal learning has been commonly employed as a measure of perseveration and, in many behavioral tasks, has been found to be dependent upon intact orbitofrontal cortex (OFC) function [4-8]. Conversely, the acquisition of well-trained stimulus-response contingencies does not require the OFC, and is more reliant on subcortical structures such as the dorsal striatum (dS) [9].

The *N*-methyl-$_D$aspartate receptor (NMDAR) is posited to be an important molecular mechanism subserving cortically-mediated processes, such as reversal learning, given its critical role in learning and various forms of synaptic plasticity linked to learning [10-14]. The GluN2B NMDAR subunit is highly expressed during development but is also selectively distributed in the adult rodent forebrain regions, including the cortex and hippocampus [15-17]. GluN2B-containing NMDARs appear to play a unique role in cortically-mediated behaviors that can be distinguished from the contribution of other types, such as GluN2A-containing NMDAR heteromers [18]. Furthermore, genetic alterations in GluN2B-containing NMDAR's C-terminus signaling domain, which alters downstream signaling and expression, have recently been associated with neuropsychiatric disorders characterized by deficits in executive control [19].

In rodents, gene deletion, age-related loss or decreased tyrosine phosphorylation of GluN2B impairs cortical plasticity and hippocampal and related forms of learning [20-23], while transgenic GluN2B overexpression or decreased GluN2B degradation was reported to enhance learning and hippocampal long-term potentiation (LTP) [24, 25].

While prior work provides compelling evidence that cortical GluN2B-containing receptors play a critical role in reversal learning, the neural underpinnings of this function are unclear. We have previously shown that selective deletion of GluN2B in cortical or CA1 hippocampal principal neurons impairs reversal (and not initial discrimination) learning and this effect can be recapitulated by microinfusion of a GluN2B antagonist into the OFC [26]. In contrast, deletion of GluN2B restricted to GABAergic interneurons significantly impaired the ability to learn an initial pairwise discrimination [27]. One outstanding question is whether GluN2B acts to support reversal learning via regulating neuronal activity locally, at the level of cortex, or whether its impact is manifest more broadly, through integrating neural activity across cortical and subcortical systems. Here, we combined a touchscreen-based reversal learning paradigm with *in vivo* electrophysiological recordings to measure neuronal activity and local field potentials (LFPs) simultaneously in the OFC and dS of mice with corticohippocampal GluN2B deletion. We found that, in the absence of the normal contribution from GluN2B-containing NMDARs, the coordinated recruitment of these brain regions during reversal learning was profoundly aberrant, whereas local OFC activity was left largely intact. Our findings demonstrate the importance of GluN2B-containing NMDARs in integrating activity across neural systems to support reversal learning.

Author Manuscript Author Manuscript Author Manuscript Author Manuscript

Materials and Methods

Animals

GluN2B mutant mice were generated and backcrossed into a ~95% C57BL/6J background, as previously described [20]. Floxed mutant mice were crossed with (C57BL/6J-congenic) transgenic mice expressing Cre recombinase driven by the CaMKII promoter (T29-1 line) [28] to produce mutant mice with excision of GluN2B ($G1uN2B^{NULL}$) in dorsal CA1 of the hippocampus and throughout the cortex and non-excised floxed littermate controls ($GluN2B^{FLOX}$) (Brigman et al., 2010b; Brigman et al., 2013). Mice were bred at the University of New Mexico Health Sciences Center and housed in same-sex groupings of 2-4 per cage in a temperature- and humidity- controlled vivarium. Lighting was on a reverse 12 h light/dark cycle (lights off 0800 h) and testing was performed during the dark phase. Sixteen (16) Male mice (aged 8 weeks at the start of testing, n=8 per genotype) were slowly reduced and then maintained at ~85% free-feeding body weight to ensure motivation to work for food reward. All experimental procedures were performed in accordance with the National Institutes of Health Guide for Care and Use of Laboratory Animals and were approved by the University of New Mexico Health Sciences Center Institutional Animal Care and Use Committee.

Operant and touchscreen apparatus

All operant behavior was conducted in a chamber measuring 21.6 × 17.8 × 12.7 cm (model # ENV-307W, Med Associates, St. Albans, VT, UA), housed within a sound- and light-attenuating box (Med Associates) as previously described [29]. The standard grid floor of the chamber was covered with a solid acrylic plate to facilitate ambulation. A pellet dispenser delivering reward (14 mg dustless pellets; #F05684, BioServ, Frenchtown, NJ, USA) into a magazine, a house-light, tone generator and an ultrasensitive lever was located at one end of the chamber. At the opposite end of the chamber was a touch-sensitive screen (Conclusive Solutions, Sawbridgeworth, UK) covered by a black acrylic aperture plate allowing two 2 × 5 cm touch areas separated by 0.5 cm and located at a height of 6.5 cm from the floor of the chamber. Stimulus presentation in the response windows and touches were controlled and recorded by the K-Limbic Software Package (Conclusive Solutions).

Pre-training

Mice were habituated to the operant chamber and to eating out of the pellet magazine by being placed in the chamber for ≤30 minutes with pellets available in the magazine. Once a mouse retrieved at least 10 pellets during habituation session, it began the pre-training regimen. First, mice were trained to obtain reward by pressing a lever within the chamber on an FR1 schedule. Once a mouse showed willingness to press the lever and collect 30 rewards in a <30 minute-session, it was moved to touch training. During this stage, a lever press led to the presentation of a white (variously-shaped) stimulus in 1 of the 2 response windows (spatially pseudorandomized). The stimulus remained on the screen until a response was made. Touches in the blank response window had no effect, while a touch to the white stimulus window resulted in reward delivery, immediately cued by a tone and illumination of the magazine. Once a mouse was able to initiate, touch and retrieve 30 pellets in a <30 minute-session, it was moved to the final stage of pre-training. This stage was identical to

Author Manuscript Author Manuscript Author Manuscript Author Manuscript

touch-training except that responses at a blank window during stimulus presentation now produced a 10-second timeout, immediately signaled by illumination of the house light, to discourage indiscriminate screen responding. Errors made on this pre-training stage (as well as on discrimination and reversal, see below), were followed by correction trials in which the same stimulus and left/right position was presented until a correct response was made. Once a mouse was able to make ≥75% (excluding correction trials) of responses at a stimulus-containing window in a 30-trial session, it was moved onto discrimination testing.

Discrimination and reversal learning

Pairwise discrimination and reversal was tested as previously described [20]. Mice were first trained to discriminate 2 novel, approximately equally-luminescent stimuli, presented in a spatially pseudorandomized manner, over 30-trial sessions (5-second inter-trial interval). The stimulus designated as correct was counterbalanced across mice and genotypes. Responses at the correct stimulus window resulted in a single food reward, cued by a 1-second tone and illumination of the magazine. Responses at the incorrect stimulus window resulted in a forced timeout, signaled by illumination of the house-light. Correction trials following errors were presented with the same stimuli in the same spatial orientation until a correct response was made. Discrimination criterion was ≥85% correct responding (excluding correction trials) over 2 consecutive sessions. Reversal training began on the session after discrimination criterion was attained. Here, the designation of correct verses incorrect stimuli was reversed for each mouse.

For discrimination and reversal, the following dependent variables were analyzed: correction errors, reaction time (time from lever press initiation to screen touch) and magazine latency (time from screen touch to reward retrieval). In order to examine distinct phases of reversal (early perseverative and late learning) errors and correction errors for sessions where performance was below 50% and performance from 50% to criterion, were separately analyzed as previously described [26, 30].

To analyze use of feedback for learning, correct and incorrect responses were further categorized based on previous trial outcome: correct responses were characterized as *win-stay* (following correct response) or *lose-shift* (following an error trial), while error trials were characterized as *perseverative* (following an error trial) or *regressive* as previously described [31]. As assumptions for normality and equivalent variance were met, data were analyzed using unpaired t-tests followed by Bonferroni correction for multiple comparisons.

Microelectrode array implantation

After completing pre-training and 1 week before discrimination testing, mice were anesthetized with isoflurane and placed in a stereotaxic alignment system (Kopf Instruments, Tujunga, CA, USA) for implantation of a microelectrode array [31-33]. The array (Innovative Neurophysiology, Durham, NC, US) comprised 16 individual 35 μm-diameter tungsten microelectrodes arranged into 2 bundles of 2×4 electrodes offset by 0.725 mm. The array was implanted in an anterior to posterior configuration (150 μm row/column spacing, 1.85 mm spacing between bundles) targeting the lateral OFC and ipsilateral dS (targeting coordinates for center of array: AP +2.60, ML +0.00, DV −2.60). After allowing 7 days of

Author Manuscript Author Manuscript Author Manuscript Author Manuscript

recovery from the surgery, food restriction resumed and mice were given a post-surgery reminder to ensure retention of pre-training criterion before commencing discrimination testing.

Multi-region electrophysiological recordings

Neuronal activity was recorded using a multichannel acquisition processor (OmniPlex, Plexon, Dallas, TX, USA), as previously described [32, 33], during each of 5 sessions corresponding to a specific stage in testing: 1) the session discrimination criterion was attained, 2) the first session of reversal, 3) the third session of reversal, 4) the fourth session of reversal, and 5) the session when reversal was at chance levels (~50% correct). As no differences were previously found between performance and activity during the 1st and 2nd sessions of reversal, recording during the 2nd reversal session was omitted to reduce strain on array head caps [29, 31].

Continuous spike signals were sampled at 40 kHz and waveforms were manually sorted during recording, based on manually set voltage threshold. LFP was sampled independently from each of the 16 electrodes implanted in the OFC and dS at 1 kHz and automatically low band pass filtered at 200 Hz (Figure 1). Neuronal recording data was timestamped via TTL pulse to time of correct or error choice. At the completion of testing, array placement was verified via electrolytic lesions made by passing 100 μA through the electrodes for 20 seconds using a current stimulator (S48 Square Pulse Stimulator, Grass Technologies, West Warwick, RI, USA). Brains were collected after perfusion with 4% paraformaldehyde and 50-μm coronal sections were cut with a vibratome (Classic 1000 model, Vibratome, Bannockburn, IL, USA), then stained with cresyl violet to verify electrode placements with reference to a mouse brain atlas [34].

Single-unit analysis

Waveforms were re-sorted offline using principal component analysis of spike clusters and visual inspection of waveform and inter-spike interval <1% shorter than 2 milliseconds using Offline Sorter (Plexon Inc), as previously described (Marquardt et al., 2016). Using NeuroExplorer software (NEX Technologies, Littleton, MA, USA), data were expressed in bins of 50 milliseconds of activity averaged across correct or error trials in a given session, and organized into epochs spanning 1 second pre-event to 3 seconds post-event, based on previously identified event-responsive windows that exclude other trial events (e.g., reward collection, or trial initiation) [32, 33]. Less than 5% of neurons exhibited a baseline firing rate of >15 Hz and were excluded from analysis as potential fast-spiking interneurons. Next, firing rates were transformed (for OFC and dS data separately) to Z-scores based on the 3-second post-event activity, normalized to the 1-second pre-event baseline. All recorded units were analyzed to examine the influence of event responsive neurons in the OFC and DS over activity as a whole. The pattern of firing rate changes were examined for the period immediately following a correct or error choice (event → 1 sec post) or more distal period (1 → 3 sec.) compared to baseline using a mixed effects repeated-measures ANOVA followed by *post hoc* Tukey's tests.

Author Manuscript Author Manuscript Author Manuscript Author Manuscript

LFP phase analysis

Inter- trial phase consistency (ITPC) quantifies the variability of a frequency-specific signal at each point in time across a behavioral measure. Consistent phase, or timing, of the LFP during a behavioral task is hypothesized to be a common mechanism for synchronizing neural activity required for multiple neuronal functions [35]. ITPC values vary from 0 to 1, where 0 indicates random phases at that time-frequency point across trials, and 1 indicates identical phase values at that time-frequency point across trials. Time-frequency analyses were adapted to depth recordings from methods previously described [36] and computed using custom Matlab (TheMathWorks, Natick, MA) scripts. All LFP recordings were grounded with a cerebellar screw. Each regional bundle (OFC vs. dS) was referenced to the recording electrode most distal from the other bundle (Figure 1). All analyses were conducted independently for each electrode. Since there were no significant differences in phase coherence between electrodes within each regional bundle within a single genetic condition, data were averaged together over electrodes to characterize a single OFC and a single dS recording. Epochs aligned to time of choice, from 1 second pre-event to 3 seconds post-event were defined for every trial occurrence. ITPC is highly dependent upon trial number, therefore, mice completing less than 12 of a given event (i.e., correct or error trials), the minimum number of trials needed for an un-inflated ITPC [37], on a given session were excluded from analysis for that session. To control for uneven trial number completion between subjects and conditions, 12 randomly selected trials were used to compute ITPC and averaged over 250 permutations for an average ITPC per subject unbiased by completed trial number. Single trial data for each trial-type were convolved with a set of complex Morlet wavelets, defined as a Gaussian-windowed complex sine wave: $e^{-i2\pi f}e^{-12/(*2\sigma 2)}$, where t is time, f is frequency (from 1 to 80 Hz in 80 logarithmic spaced steps to maximize lower frequency visualization), and σ is the width of each frequency band set at $4/(2\pi f)$ [36, 37]. Inter trial phase consistency (ITPC) was quantified as the length of the average of unit-length vectors that were distributed according to their phase angles (Lachaux et al., 1999).

To meaningfully compare ITPC spectra data, nonparametric permutation shuffling of all data (genotype, subjects and sessions) to identify time-frequency region of interest (TF-ROI) that were event dependent to compare magnitude of ITPC response between factors. A linear mixed model (R, lmr4), which is robust against missing data, was used to statistically compare the ITPC magnitude resulting from averaging data values within the TF-ROI for each subject. Session was defined as a within factor, and genotype as a between factor, to determine the contribution and interaction of all dimensions of the data, via a linear mixed model ANOVA and *post hoc* Tukey's tests corrected by Bonferroni for multiple comparisons.

Analysis of neural activity between OFC and dS

We performed two separate analyses of functional connectivity between OFC and dS. First, the difference in phase angles was used to assess phase-based coupling between regions [38]= Whereas ITPC investigates phase consistency within a site over trials, inter-site phase consistency (ISPC) investigates phase consistency between two sites across trials. ISPC was calculated from the difference in phase angle between OFC and dS

Author Manuscript Author Manuscript Author Manuscript Author Manuscript

$y: ISPC_{R(t)} = \sum_{r=1}^{n} \left| e^{i(\varnothing_{xt} - \varnothing_{yt})} \right|$ where $R(t)$ was the convolved time-frequency data at each time point (t) and trial (r) [39]. Trial count control and permutations were performed as described for ITPC. Additionally, TF-ROI that represented event dependent changes in ISPC were defined, averaged per subject and statistically compared as described for ITPC.

Second, we performed a single Granger bivariate autoregression analysis for OFC→dS and dS→OFC broadband directional coupling. Due to its high time resolution, fast sampling and spatial precision intracranial LFP data are well suited for Granger autoregression analysis [40]. Analyses were adapted from the BSMART toolbox (Cui et al. 2008), the Granger autoregression connectivity analysis tool box (GCCA) [41] and Analyzing Neural Time Series Data [37]. Raw LFP data from both OFC and dS were downsampled to 200 Hz. Correct choice trials were analyzed independently on a sliding time scale from −1 sec pre-choice to +3 sec post-choice, windowed into 500 ms blocks with 250 ms overlap. The ERP was subtracted before each time segment was z-scored and detrended for improved stationarity. Mice completing less than 12 of the defined trial type were excluded from the analysis for the corresponding recording session. Prior to Granger autoregression, model order was calculated on utilizing Bayesian Information Criterion (BIC) independently for each trial type, session, treatment and subject [42]. Average model order was rounded to the nearest whole number for a final order number of 7, allowing for 35 ms of past data to be incorporated in to the Granger prediction. This model order is similar to those previously published with intracranial LFP recording {Zavala, 2014 #543}. Granger autoregression defined as, $C = ln\left(\frac{\sigma(Ex)}{\sigma(Exy)}\right)$ with $\sigma(Ex)$ and $\sigma(Ex)$ variance error terms from univariate and bivariate autoregression models, respectively, was calculated over each time window utilizing the BIC defined model order. Autoregression coefficients were convolved with complex sine waves across focused logspaced frequencies from 1 to 10 Hz and applied to the model error variance via transfer function for analysis across frequency and time [43].

While differences in Granger autoregression magnitude have been shown to be distinguishable between low-frequencies [44] broad frequency range TF-ROI were defined based on event driven changes in Granger magnitude for conservative Granger autoregression analysis. TF-ROI boundaries were used to calculate average Granger values within each subject, session and region for statistical comparison. A linear mixed model (R, lmr4), which is robust against missing data, was used to fit the repeated cross-session ROI averages with session as a within factor, and treatment as a between factor, to determine the contribution and interaction of all dimensions of the data. Statistically significant contributions of factors and interactions were determined by ANOVA and post-hoc Bonferroni's tests.

Results

Impaired reversal learning in GluN2B^{NULL} mice

G1uN2B^{NULL} showed similar performance to GluN2B^{FLOX} control mice during discrimination and performance appeared unaffected by the multichannel electrode array implants (t(14)=2.16, p=.17; Figure 2A). However, in agreement with our previous results

Author Manuscript Author Manuscript Author Manuscript Author Manuscript

GluN2B^{NULL} mice made significantly more correction errors across the entire reversal than controls (t(14)=7.31, p=.017; Figure 2B). There was no significant difference between session on which groups achieved 50% correct (t=.721, df=14, p=.4825; GluN2B^{FLOX}=6.25±.861; G1uN2B^{NULL}=7.13±.85). Analysis of correction errors made during early (<50% correct; t=5.23, df=14, p=.039) versus later (≥50% correct; t(14)=9.28, p=.010) reversal revealed that GluN2B^{NULL} made significantly more errors during both phases (Figure 2C). Secondary measures showed that genotypes did not differ on latency to make a choice response or enter the reward magazine, during discrimination (choice: t=1.82, df=14, p=.08: magazine: t=1.28, df=14, p=.22) on either perseverative (≥50% correct choice: t=1.51, df=14, p=.15; magazine: t=.61, df=14, p=.55) or learning phase (≥50% correct choice: t= 1.81, df=14, p=.10; magazine: t=1.16, df=14, p=.27) of reversal (Figure 2A-D).

Analysis of percent correct responses during each of the 5 reversal recording sessions (final session of discrimination, 1st, 3rd, 4th sessions after the start of reversal, as well as the 1st session at 50% accuracy) revealed that GluN2B^{NULL} did not differ from controls on any session (genotype effect: $F_{1,56}$=.35, p=.34; Figure 3A). Analysis of correct response type based on previous response showed no significant effect of genotype on *Win-Stay* trials (genotype effect: $F_{1,56}$=0.07, p=.90; Figure 3B) or *Lose-Shift* responses (genotype effect: $F_{1,56}$=0.44, p=.84; Figure 3C) although both trial types varied significantly across recording sessions (*Win-Stay* session effect: $F_{1,56}$=108.6, p=.0004; *Lose-Shift* session effect $F_{1,56}$=128.8, p=.0001). However, GluN2B^{NULL} mice made significantly more total errors during the 3rd and 4th sessions, compared to controls (genotype effect: $F_{1,56}$=6.22, p=.034; session effect: $F_{4,56}$=29.02, p=.0001; genotype x session: $F_{4,56}$=3.42, p=.017, Figure 3D). Analysis of error type based on previous response showed that GluN2B^{NULL} made significantly more Perseverative (error → error) responses on the 3rd and 4th reversal session compared to controls (genotype effect: $F_{1,56}$=6.86, p=.027; session effect $F_{4,56}$=26.2, p=.0001; genotype x session: $F_{4,56}$=2.85, p=.038; Figure 3E). No significant differences on Regressive errors (correct → error) were seen between genotype (genotype: $F_{1,56}$=0.42, p=.97; Figure 3F) although this error type also varied by session (session effect $F_{4,56}$=93.2, p=.0007). No significant differences by genotype were seen on choice latency (genotype effect: $F_{1,56}$=2.60, p==.14) or magazine latency (genotype effect: $F_{1,56}$=4.18, p=.09) at any session (data not shown).

OFC neuronal activity in GluN2B^{NULL} mice

Spike firing activity was analyzed across 504 putative OFC pyramidal neurons in GluN2B^{NULL} and GluN2B^{FLOX} controls (Figure 4A). Genotypes did not differ in pre-choice baseline firing rate (Figure 4B). OFC neuronal activity increased following a correct choice response irrespective of genotype (main effect of time: Disc: $F_{1,27}$=6.18, p=.0001; Rev S1: $F_{1,27}$=4.51, p=.0001; Rev S3: $F_{1,27}$=4.79, p=.0001; Rev Chance: $F_{1,27}$=9.61, p=.0001; Figure 4C). However, at the Chance Reversal stage there was a significant interaction between genotypes during reward-cue tone presentation (genotype x time: $F_{1,27}$=2.44, p=.0004) and across the entire cue-choice epoch (genotype x time: $F_{1,27}$=6.18. p=.0002). due to higher OFC neuronal activity in GluN2B^{NULL} mice than controls during the cue, and a lesser response in the post-cue-to-reward period (Figure 4C).

Author Manuscript Author Manuscript Author Manuscript Author Manuscript

There was altered neuronal OFC activity in the period following an error during the 1st (main effect of time: $F_{1,59}$=1.51, p=.0069) and the Chance (main effect of time: $F_{1,59}$=2.51. p=.0001) reversal sessions (Figure 4D). Activity was reduced during this period in GluN2B^{NULL} mice, relative to controls, specifically during 1st to 3rd reversal sessions, but was significantly increased later in reversal, during the 4th session and then became similar to controls by the chance reversal session (genotype x time: Disc: $F_{1,59}$=1.64, p=.0014; Rev S1: $F_{1,59}$=2.02, p=.0001; Rev S3: $F_{1,59}$= 1.65, p=.00l2; Rev Chance: $F_{1,59}$=1.39, p=.026).

dS neuronal activity in GluN2B^{NULL} mice

Activity was analyzed across 192 putative medium spiny dS neurons in GluN2B^{NULL} and GluN2B^{FLOX} controls (Figure 5A). No genotype difference was evident in baseline firing rate (Figure 5B). Analysis of dS activity revealed that firing significantly increased following a correct choice response during all recording sessions (main effect of time: Disc: $F_{1,59}$=3.59, p=.0001; Rev S1: $F_{1,59}$=2.58, p=.0001; Rev S3: $F_{1,59}$=4.98, p=.0001; Rev S4: $F_{1,59}$=4.37, p=.0001; Rev Chance: $F_{1,59}$=6.34, p=.0001; Figure 5C). There was a significant interaction between genotypes and time for activity during the reward-cue period on the 3rd (interaction: $F_{1,19}$=1.76, p=.023) and chance reversal (interaction: $F_{1,19}$=1.65, p=.039) sessions (Figure 5C).

dS activity following an error was increased on the 1st-4th reversal sessions (main effect of time: Rev S1: $F_{1,59}$=3.48, p=.0001; Rev S3: $F_{1,59}$=1.94, p=.0001; Rev S4: $F_{1,59}$=2.73, p=. 0001), regardless of genotype. At the chance reversal stage, both genotypes also showed increased firing following an error. However, GluN2B^{NULL} mice showed decreased firing relative to controls (main effect of time: $F_{1,59}$=1.41, p=.022; main effect of genotype: $F_{1,59}$=5.73, p=.021; Figure 5D).

Regional ITPC in GluN2B^{NULL} mice

ITPC analysis incorporating OFC and dS activity across all sessions and genotypes identified a TF-ROI (time-frequency area of interest) in the delta band (δ, 1-4 Hz) at the time of associative tone cessation. In GluN2B^{FLOX} control mice, OFC and dS delta ITPC showed similar patterns to associative cue cessation across sessions in the identified TF-ROI. During early reversal, ITPC magnitude increased across sessions compared to discrimination, peaking to be significantly higher than all other sessions during reversal S4, before decreasing to discrimination levels upon re-attainment of chance criterion (Main effect of session $F_{1,695}$=16.09, p=.0001; post-hoc Bonferroni's, Disc p=.0001, Rev S1 p=.0001, Rev S3 p=.0001, Chance p=.0001; Figure 6D-F & 7D-F).

G1uN2B^{NULL} mice, compared to control GluN2B^{FLOX}, had increased levels of ITPC in both the OFC and dS during discrimination and reversal S1 to an unexpected correct response (Main effect of treatment $F_{1,695}$=17.06, p=.0001; Treatment x Session $F_{1,695}$=3.63, p=.006; post-hoc Bonferroni's Disc p=.0002, Rev S1 p=.0005, Figure 6A-B & 7A-B). ITPC levels in GluN2B^{NULL} did not significantly differ from control levels during reversal S3 and S4 (Figure 6C-D, 7C-D). However, OFC and dS ITPC remained significantly elevated in GluN2B^{NULL} mice into chance reversal as control GluN2B^{FLOX} ITPC decreased in the OFC and dS (post-hoc Bonferroni's Chance p=.0005; Figure 7E-F & 7E-F).

Author Manuscript Author Manuscript Author Manuscript Author Manuscript

Although patterns of ITPC response were similar between regions, across sessions and within both genotypes, dS ITPC magnitude was significantly greater than in the OFC (Main effect of Region $F_{1,695}$=28.85, p=.0001; Figure 6F & 7F). Additionally, there were no significant correlations between OFC or dS ITPC and latency to retrieve reward in either GluN2B^{NULL} or control GluN2B^{FLOX} mice, suggesting that ITPC changes were not significantly influenced by motor movements towards the reward magazine (GluN2B^{FLOX} OFC: R^2= .458; p=.301; GluN2B^{NULL} OFC: R^2= −.358; p=.451; GluN2B^{FLOX}dS: R^2= −.059; p=.900; GluN2B^{NULL} dS: R^2= −.312; p=.451).

While phase-based and power-based derivations of LFP waveforms are mathematically separable, they tend to co-vary and may influence each other [45]. To examine the independence of these phenomena, we aligned dB change power plots to the ITPC for comparison between peak ITPC response and large power fluctuations. No consistent statistically significant TF-ROI emerged across reversal sessions for dB change from baseline power, suggesting that changes in power were not strongly linked to session specific behaviors, moreover there were no statistically significant differences between GluN2B^{FLOX} and GluN2B^{NULL} power responses (Figure 6G & 7G).

OFC-dS connectivity in GluN2B^{NULL} mice

The investigation of phase consistency between OFC and dS (ISPC) revealed significant increases in OFC-dS coupling in both genotypes during the 4th reversal session compared to all other sessions in both GluN2B^{NULL} and control GluN2B^{FLOX} mice during correct choices only (Main effect of session $F_{4,348}$=7.86, p=.0001; Figure 8D&F). In GluN2B^{NULL}, OFC-dS ISPC was significantly increased across reversal sessions, compared to GluN2B^{FLOX} (Main effect of genotype $F_{1,348}$=74.43, p=.04; Figure 8). ISPC was most robustly increased during reversal sessions 1, 4 and chance; however, session differences failed to reach significance (p=.079).

To further analyze OFC-dS functional connectivity utilizing robust autoregressive analysis, we performed Granger prediction analysis. We defined two time points, choice and associative cue cessation in which Granger showed event-dependent response during behavioral trials. However, connectivity responses across session and genotypes did not significantly vary based on these and therefore data was collapsed between the time points for one Granger prediction value. In both genotypes, information transfer was significantly greater from OFC to dS versus the dS to OFC direction across sessions (Main effect of direction $F_{1,1389}$=5.22, p=.02; Main effect of Session $F_{4,1389}$=2.85, p=.02; Figure 9). OFC to dS directional signaling was decreased in GluN2B^{NULL} mice across each session of early reversal compared to control GluN2B^{FLOX}; however, these decreases did not reach significance. However, upon reattainment of chance performance during reversal OFC to dS signaling was significantly increased in GluN2B^{NULL} mice (Main effect of treatment $F_{1,413}$=4.61, p=.03; Main effect of direction $F_{1,413}$=12.76, p=.0004; Treatment x Direction Interaction $F_{1,413}$=7.32, p=.007; Figure 9E-F). Analysis of indirect information flow from the DS to OFC revealed elevated directional signaling in GluN2B^{NULL} during discrimination and reversal S1 and S3, although overall signaling was low in both genotypes and these changes were not significant.

Author Manuscript Author Manuscript Author Manuscript Author Manuscript

Discussion

Consistent with previous findings, cortico-hippocampal GluN2B mutant mice demonstrated intact associative learning but a significant impairment in early reversal learning. We found that GluN2B^{NULL} mice had specific reductions in cortical and striatal spike-firing activity, particularly during early reversal. However, the most robust effects of cortico-hippocampal GluN2B loss were seen in the regional coordination and functional connectivity between OFC and dS. Our data suggest a critical role for GluN2B-containing NMDAR in the coordination of oscillatory timing from the OFC to dS, and that this coordination may be required to efficiently reverse previously learned responses.

There is strong evidence for the role of GluN2B in flexible behavior as systemic administration of a GluN2B-selective antagonist impairs reversal of cued operant responses and response-shifting to an egocentric strategy [46]. We previously reported that GluN2B^{NULL} mice demonstrate normal visual discrimination learning but are selectively impaired on reversal, with GluN2B antagonism of the OFC sufficient to replicate this deficit [26]. Here we found that GluN2B^{NULL} mice tethered for *in vivo* recording, again, had normal discrimination learning, but significant increases in perseverative responding, primarily during the early phase of reversal as seen by total errors and error-type analysis. Untethered GluN2B^{NULL} mice in previous experiments showed an increase in reversal errors during the later phase, which did not reach significance [32]. Here, the increase in reversal learning errors in GluN2B^{NULL} mice was small but significant during later reversal. Examination of response latencies during recording showed that time from initiation to choice was increased compared to non-tethered animals. Similarly, time to collect reward following a correct response was elevated above what was previously seen, regardless of genotype. While other factors may be at play, it may be that the additional stress of tethering for recording led to preservation in GluN2B^{NULL} mice extending into the chance phase, exaggerating the previously reported increases.

Loss of corticohippocampal GluN2B alters both cortical and striatal firing activity

Spike-firing rates following correct responses in GluN2B^{FLOX} closely followed the pattern previously seen in C57BL/6J mice, robustly increasing when responses were well-learned and decreasing during early reversal. While significantly faster increases occurred during chance in GluN2B^{NULL} animals, the pattern of OFC firing to correct responses was only significantly altered in GluN2B^{NULL} mice during chance reversal. More strikingly, post-error firing rates were significantly altered in GluN2B^{NULL} across all sessions of early reversal. The firing pattern of OFC neurons following correct and error trials plays a unique role in tracking and encoding the value of the previous response and is sensitive to NMDAR blockade [47]. In non-human primates, OFC spike-firing responses switch target responding within several trials [48], while in mice, this change is much slower, and reversal takes several sessions [31]. Firing of OFC pyramidal neurons following correct responses is increased when the expected value of the choice matches the outcome during criterion, and is reduced when expectancies are not met during early reversal [49-52]. In a complementary manner, firing following an error significantly increases when the absence of reward is unexpected during early reversal, and decreases following the perseverative phase [53].

Author Manuscript Author Manuscript Author Manuscript Author Manuscript

While GluN2B^{NULL} mice showed a pattern of slow building of OFC firing to newly rewarded choices that matched control animals, signaling following a learned choice that failed to produce a reward was significantly decreased; indicating delayed OFC neuron activity may be contributing to maladaptive perseveration. While behavioral deficits in GluN2B^{NULL} mice were restricted to cortically-mediated actions, alterations in neuronal firing were not restricted to the cortex. Loss of cortico-hippocampal GluN2B led to alterations in firing rate in the dS with significant alterations in firing following a correct choice both during early reversal session 2 and after any choice type at chance. Single unit local activity suggests delayed OFC activity allows for dS to drive perseverative responding during early reversal. However, by the end of the perseverative phase OFC activity is recruited allowing for a reversal of behavior. Based on this data, we hypothesize that strong coordinated network activity between cortical and striatal regions is necessary for optimal behavioral flexibility, which has a delayed peak with loss of GluN2B in the cortex and hippocampus.

Oscillatory coordination is increased in GluN2B^{NULL}mice

Analysis of oscillatory coordination supports a role for altered OFC activity, with GluN2B^{NULL} mice showing significant increases in OFC phase consistency response during early reversal, where perseveration is high. This is followed by an inappropriately prolonged OFC ITPC response while new contingencies are being learned. Alterations in low-frequency oscillation coordination marking a correct choice is thought to be essential for encoding reward anticipation in the OFC during discrimination and reversal, but has previously only been shown in the rat [54]. Our data suggest loss of GluN2B leads to inappropriately robust phase alignment to a previously unrewarded stimulus that subsequently leads to perseveration and prolonged OFC timing discrepancies into the learning phase of reversal. Reduced OFC single-unit firing rates, and aberrant local LFP phase alignment to a previously unrewarded choice during the first session of reversal suggests that loss of GluN2B-containing NMDARs may lead to a non-specific network response that disrupts outcome tracking when contingencies change and leads to perseverative response patterns.

Although the relationship between any individual unit firing and local LFP is not deterministic [55], local oscillations have been shown to entrain local firing [56-58]. Given their slower channel kinetics, lower open probabilities and higher sensitivity to glutamate, GluN2B-containing NMDAR are a strong candidate mechanism for controlling timing of neuronal activity to coordinate with oscillatory signaling [59]. Studies suggest that the GluN2A/GluN2B ratio controls the threshold required to induce plasticity [60], with learning or sensory input increasing both the ratio and the threshold of plasticity induction [61, 62]. In contrast, decreases in GluN2A/GluN2B ratio allow the induction of plasticity and are thought to be required to make associations more labile and modify existing behavioral responses [63]. These studies suggest the absence of cortical GluN2B in the OFC in our model increases the GluN2A/GluN2B ratio, reducing plasticity and the ability of individual units to entrain with local oscillations.

Author Manuscript Author Manuscript Author Manuscript Author Manuscript

Alterations in oscillatory activity were not restricted to the cortex, the site of GluN2B knockdown. Loss of cortico-hippocampal GluN2B significantly increased striatal delta ITPC following a correct response during early reversal. These striatal changes closely mirrored, and were even more pronounced, than the increased OFC ITPC in mutant mice. The OFC forms a circuit with downstream striatal regions involved to facilitate discrimination and subsequent alterations in behavior [64-66] including the dS. While OFC connections to the dS are less robust than ventral areas of the striatum, dS specifically facilitates the transition from early to well-learned behaviors and loss of dS function impairs efficient visual discrimination learning [9, 32, 67]. Increased and sustained firing, and increases in striatal dendritic morphology, have been shown to speed the development of an automatized associative response [33]. It has recently been shown that activation of lateral aspects of dS responsible for later stimulus-response behavior may interfere with the early phase of associative learning [68]. As in the OFC, the coordinated activity of the dS was increased in GluN2B^{NULL} mice during early reversal. Increased striatal firing together with increased coordination as measured by phase alignment support the hypothesis that loss of cortico-hippocampal GluN2B results in sustained striatal signaling during reversal that extends the perseverative period by driving responding to the previously rewarded choice. Our data suggest that the loss of cortical-hippocampal GluN2B mice are committed to a maladaptive behavioral pattern by continued dS activity, and take longer to activate OFC local network activity to exert top down control. Together with significant changes OFC firing and coordination, this indicates that loss of cortical GluN2B both decreased the ability of the OFC to exert top-down control locally and facilitated hyperactivity within the dS, resulting in a phenotype that required extended experience with feedback cues in order to alter behavioral patterns during the reversal task. A loss of local OFC coordination and the inability to efficiently exert top-down control led us to hypothesize a further disruption of OFC to dS communication.

OFC to dS signaling is aberrant after cortico-hippocampal GluN2B deletion

Simultaneous recording of both regions in behaving mice allowed for further analysis of functional connectivity between the OFC and dS to examine if loss of cortical GluN2B altered coordination as suggested by the waveform and LFP phase analysis. GluN2B^{NULL} mice showed increased ISPC between the OFC and dS during early reversal, although the increase was not significant. Similarly, Granger prediction showed that while control mice had robust OFC to dS directional signaling that increased during early reversal, GluN2B^{NULL} mice had aberrantly increased functional connectivity during late reversal. Cortico-striatal circuits are hypothesized to require coordinated activity via oscillatory coordination to facilitate common functions [69, 70]. Crosstalk between these regions is likely necessary to perform well-learned actions while monitoring and signaling changes in outcomes of these actions. Increases in ISPC seen in mutant mice may represent an aberrant “locking” of OFC-dS activity. Together with delayed increases in OFC event-responsive neuron firing and increased phase coherence during the first session of reversal data suggest that GluN2B cortical loss leads to an activity that occludes early cortical signaling required to update reward expectancies. Delayed OFC-dS network recruitment ultimately leads to a normalization of behavior late in the perseverative phase. Although ISPC was phase-specific and Granger Causality used a broad frequency complex-valued LFP, both models support the

Author Manuscript Author Manuscript Author Manuscript Author Manuscript

conclusion that GluN2B loss in the cortex interrupts cortical-striatal communication during reversal learning.

Together with waveform and phase alignment data, these analyses lend support to the hypothesis that GluN2B may play a critical role in proper synchronization of cortical-striatal activity required to signal when previously learned expectancies have changed. While further studies are needed to determine the extent to which oscillatory timing is necessary for efficient reversal, it is well established that loss of GluN2B subunits impairs plasticity, both in the cortex and other regions [20-23]. While not as temporally specific as targeted antagonism, our current genetic knockdown data suggest loss of GluN2B may drive perseverative patterns of responding by decreasing the ability of the OFC to coordinate its activity sufficiently to signal downstream regions and update previously learned patterns of behavior.

The current study provides new evidence that GluN2B-containing NMDARs are required for the induction of appropriate signaling in the cortex when choice values change. While loss of GluN2B in the cortex has effects on the firing rate of pyramidal neurons, it leads to both significant increases and delays in low-frequency coordination and reduction in OFC to dS functional connectivity. Beyond direct cortical effects, loss of GluN2B led to significant increases in phase consistency in the dS, and aberrantly timed OFC to dS functional connectivity. These findings provide the first evidence of how loss of a critical population of NMDARs can alter the coordinated action of the cortex and its communication with the basal ganglia.

Acknowledgements

We are very grateful to Shih-Chieh (CJ) Lin for his insightful comments and assistance with this manuscript. This work was supported by the NIAAA Intramural Research Program and grants 1K22AA020303-01, 1P50AA022534-01 and 5T32AA014127e13.

References

[1]. Gilmour G, Arguello A, Bari A, Brown VJ, Carter C, Floresco SB, Jentsch DJ, Tait DS, Young JW, Robbins TW, Measuring the construct of executive control in schizophrenia: defining and validating translational animal paradigms for discovery research, Neurosci Biobehav Rev, 37 (2013) 2125–2140. [PubMed: 22548905]

[2]. Brennan AR, Arnsten AF, Neuronal mechanisms underlying attention deficit hyperactivity disorder: the influence of arousal on prefrontal cortical function, Ann N Y Acad Sci, 1129 (2008) 236–245. [PubMed: 18591484]

[3]. Evans SW, Brady CE, Harrison JR, Bunford N, Kern L, State T, Andrews C, Measuring ADHD and ODD symptoms and impairment using high school teachers' ratings, J Clin Child Adolesc Psychol, 42 (2013) 197–207. [PubMed: 23215533]

[4]. Hamilton DA, Brigman JL, Behavioral flexibility in rats and mice: Contributions of distinct frontocortical regions, Genes, brain, and behavior, DOI 10.1111/gbb.12191(2015).

[5]. Izquierdo A, Brigman JL, Radke AK, Rudebeck PH, Holmes A, The neural basis of reveral learning: An updated perspective, Neuroscience, (2016).

[6]. Kennerley SW, Behrens TE, Wallis JD, Double dissociation of value computations in orbitofrontal and anterior cingulate neurons, Nat Neurosci, 14 (2011) 1581–1589. [PubMed: 22037498]

[7]. Stalnaker TA, Cooch NK, Schoenbaum G, What the orbitofrontal cortex does not do, Nat Neurosci, 18 (2015) 620–627. [PubMed: 25919962]

Author Manuscript Author Manuscript Author Manuscript Author Manuscript

[8]. Rudebeck PH, Saunders RC, Prescott AT, Chau LS, Murray EA, Prefrontal mechanisms of behavioral flexibility, emotion regulation and value updating, Nat Neurosci, 16 (2013) 1140–1145. [PubMed: 23792944]

[9]. Yin HH, Mulcare SP, Hilario MR, Clouse E, Holloway T, Davis MI, Hansson AC, Lovinger DM, Costa RM, Dynamic reorganization of striatal circuits during the acquisition and consolidation of a skill, Nat Neurosci, 12 (2009) 333–341. [PubMed: 19198605]

[10]. Bannerman DM, Rawlins JN, Good MA, The drugs don't work-or do they? Pharmacological and transgenic studies of the contribution of NMDA and GluR-A-containing AMPA receptors to hippocampal-dependent memory, Psychopharmacology (Berl), 188 (2006) 552–566. [PubMed: 16676163]

[11]. Chadman KK, Watson DJ, Stanton ME, NMDA receptor antagonism impairs reversal learning in developing rats, Behav Neurosci, 120 (2006) 1071–1083. [PubMed: 17014258]

[12]. Cotman CW, Monaghan DT, Ganong AH, Excitatory amino acid neurotransmission: NMDA receptors and Hebb-type synaptic plasticity, Annu Rev Neurosci, 11 (1988) 61–80. [PubMed: 2452598]

[13]. Malenka RC, Bear MF, LTP and LTD: an embarrassment of riches, Neuron, 44 (2004) 5–21. [PubMed: 15450156]

[14]. Mikics E, Toth M, Biro L, Bruzsik B, Nagy B, Haller J, The role of GluN2B-containing NMDA receptors in short- and long-term fear recall, Physiol Behav, 177 (2017) 44–48. [PubMed: 28400283]

[15]. Akazawa C, Shigemoto R, Bessho Y, Nakanishi S, Mizuno N, Differential expression of five N-methyl-D-aspartate receptor subunit mRNAs in the cerebellum of developing and adult rats, J Comp Neurol, 347 (1994) 150–160. [PubMed: 7798379]

[16]. Monyer H, Burnashev N, Laurie DJ, Sakmann B, Seeburg PH, Developmental and regional expression in the rat brain and functional properties of four NMDA receptors, Neuron, 12 (1994) 529–540. [PubMed: 7512349]

[17]. Frank RA, Komiyama NH, Ryan TJ, Zhu F, O'Dell TJ, Grant SG, NMDA receptors are selectively partitioned into complexes and supercomplexes during synapse maturation, Nat Commun, 7 (2016) 11264. [PubMed: 27117477]

[18]. Ryan TJ, Kopanitsa MV, Indersmitten T, Nithianantharajah J, Afinowi NO, Pettit C, Stanford LE, Sprengel R, Saksida LM, Bussey TJ, O'Dell TJ, Grant SG, Komiyama NH, Evolution of GluN2A/B cytoplasmic domains diversified vertebrate synaptic plasticity and behavior, Nat Neurosci, 16 (2013) 25–32. [PubMed: 23201971]

[19]. Liu S, Zhou L, Yuan H, Vieira M, Sanz-Clemente A, Badger JD 2nd, Lu W, Traynelis SF, Roche KW, A Rare Variant Identified Within the GluN2B C-Terminus in a Patient with Autism Affects NMDA Receptor Surface Expression and Spine Density, J Neurosci, 37 (2017) 4093–4102. [PubMed: 28283559]

[20]. Brigman JL, Wright T, Talani G, Prasad-Mulcare S, Jinde S, Seabold GK, Mathur P, Davis MI, Bock R, Gustin RM, Colbran RJ, Alvarez VA, Nakazawa K, Delpire E, Lovinger DM, Holmes A, Loss of GluN2B-containing NMDA receptors in CA1 hippocampus and cortex impairs long-term depression, reduces dendritic spine density, and disrupts learning, J Neurosci, 30 (2010) 4590–4600. [PubMed: 20357110]

[21]. Duffy S, Labrie V, Roder JC, D-Serine Augments NMDA-NR2B Receptor-Dependent Hippocampal Long-Term Depression and Spatial Reversal Learning, Neuropsychopharmacology, 33 (2008) 1004–1018. [PubMed: 17625504]

[22]. Higgins GA, Ballard TM, Enderlin M, Haman M, Kemp JA, Evidence for improved performance in cognitive tasks following selective NR2B NMDA receptor antagonist pre-treatment in the rat, Psychopharmacology, 179 (2005) 85–98. [PubMed: 15759152]

[23]. von Engelhardt J, Doganci B, Jensen V, Hvalby O, Gongrich C, Taylor A, Barkus C, Sanderson DJ, Rawlins JN, Seeburg PH, Bannerman DM, Monyer H, Contribution of hippocampal and extra-hippocampal NR2B-containing NMDA receptors to performance on spatial learning tasks, Neuron, 60 (2008) 846–860. [PubMed: 19081379]

Author Manuscript Author Manuscript Author Manuscript Author Manuscript

[24]. Hawasli AH, Benavides DR, Nguyen C, Kansy JW, Hayashi K, Chambon P, Greengard P, Powell CM, Cooper DC, Bibb JA, Cyclin-dependent kinase 5 governs learning and synaptic plasticity via control of NMDAR degradation, Nat Neurosci, 10 (2007) 880–886. [PubMed: 17529984]

[25]. Tang YP, Shimizu E, Dube GR, Rampon C, Kerchner GA, Zhuo M, Liu G, Tsien JZ, Genetic enhancement of learning and memory in mice, Nature, 401 (1999) 63–69. [PubMed: 10485705]

[26]. Brigman JL, Daut RA, Wright T, Gunduz-Cinar O, Graybeal C, Davis MI, Jiang Z, Saksida LM, Jinde S, Pease M, Bussey TJ, Lovinger DM, Nakazawa K, Holmes A, GluN2B in corticostriatal circuits governs choice learning and choice shifting, Nature Neuroscience, 16 (2013) 1101–1110. [PubMed: 23831965]

[27]. Brigman JL, Daut RA, Saksida L, Bussey TJ, Nakazawa K, Holmes A, Impaired discrimination learning in interneuronal NMDAR-GluN2B mutant mice, Neuroreport, 26 (2015) 489–494. [PubMed: 25968910]

[28]. Fukaya M, Kato A, Lovett C, Tonegawa S, Watanabe M, Retention of NMDA receptor NR2 subunits in the lumen of endoplasmic reticulum in targeted NR1 knockout mice, Proc Natl Acad Sci U S A, 100 (2003) 4855–4860. [PubMed: 12676993]

[29]. Marquardt K, Sigdel R, Caldwell K, Brigman JL, Prenatal ethanol exposure impairs executive function in mice into adulthood, Alcohol Clin Exp Res, 38 (2014) 2962–2968. [PubMed: 25581651]

[30]. Brigman JL, Mathur P, Harvey-White J, Izquierdo A, Saksida LM, Bussey TJ, Fox S, Deneris E, Murphy DL, Holmes A, Pharmacological or Genetic Inactivation of the Serotonin Transporter Improves Reversal Learning in Mice, Cereb Cortex, (2010).

[31]. Marquardt K, Sigdel R, Brigman JL, Touch-screen visual reversal learning is mediated by value encoding and signal propagation in the orbitofrontal cortex, Neurobiol Learn Mem, 139 (2017) 179–188. [PubMed: 28111339]

[32]. Brigman JL, Daut RA, Wright T, Gunduz-Cinar O, Graybeal C, Davis MI, Jiang Z, Saksida LM, Jinde S, Pease M, Bussey TJ, Lovinger DM, Nakazawa K, Holmes A, GluN2B in corticostriatal circuits governs choice learning and choice shifting, Nat Neurosci, 16 (2013) 1101–1110. [PubMed: 23831965]

[33]. DePoy L, Daut R, Brigman JL, MacPherson K, Crowley N, Gunduz-Cinar O, Pickens CL, Cinar R, Saksida LM, Kunos G, Lovinger DM, Bussey TJ, Camp MC, Holmes A, Chronic alcohol produces neuroadaptations to prime dorsal striatal learning, Proc Natl Acad Sci U S A, 110 (2013) 14783–14788. [PubMed: 23959891]

[34]. Paxinos KBJ, Franklin G, The mouse brain in stereotaxic coordinates 2nd ed., Academic Press, London, 2001.

[35]. Womelsdorf T, Fries P, Neuronal coherence during selective attentional processing and sensory-motor integration, J Physiol Paris, 100 (2006) 182–193. [PubMed: 17317118]

[36]. Cavanagh JF, Cohen MX, Allen JJ, Prelude to and resolution of an error: EEG phase synchrony reveals cognitive control dynamics during action monitoring, J Neurosci, 29 (2009) 98–105. [PubMed: 19129388]

[37]. Cohen MX, Analyzing Neural Time Series Data Theory and Practice Preface, Iss Clin Cogn Neurop, (2014) Xvii–Xviii.

[38]. Fries P, A mechanism for cognitive dynamics: neuronal communication through neuronal coherence, Trends Cogn Sci, 9 (2005) 474–480. [PubMed: 16150631]

[39]. Vinck M, van Wingerden M, Womelsdorf T, Fries P, Pennartz CM, The pairwise phase consistency: a bias-free measure of rhythmic neuronal synchronization, Neuroimage, 51 (2010) 112–122. [PubMed: 20114076]

[40]. Barnett L, Seth AK, The MVGC multivariate Granger causality toolbox: a new approach to Granger-causal inference, J Neurosci Methods, 223 (2014) 50–68. [PubMed: 24200508]

[41]. Seth AK, A MATLAB toolbox for Granger causal connectivity analysis, J Neurosci Methods, 186 (2010) 262–273. [PubMed: 19961876]

[42]. Schwarz G, Estimating the Dimension of a Model, The Annals of Statistics 6(1978) 461–464.

[43]. Cui J, Xu L, Bressler SL, Ding M, Liang H, BSMART: a Matlab/C toolbox for analysis of multichannel neural time series, Neural Netw, 21 (2008) 1094–1104. [PubMed: 18599267]

Author Manuscript Author Manuscript Author Manuscript Author Manuscript

[44]. Zavala BA, Tan H, Little S, Ashkan K, Hariz M, Foltynie T, Zrinzo L, Zaghloul KA, Brown P, Midline frontal cortex low-frequency activity drives subthalamic nucleus oscillations during conflict, J Neurosci, 34 (2014) 7322–7333. [PubMed: 24849364]

[45]. van Diepen RM, Mazaheri A, The Caveats of observing Inter-Trial Phase-Coherence in Cognitive Neuroscience, Sci Rep, 8 (2018) 2990. [PubMed: 29445210]

[46]. Dalton GL, Ma LM, Phillips AG, Floresco SB, Blockade of NMDA GluN2B receptors selectively impairs behavioral flexibility but not initial discrimination learning, Psychopharmacology (Berl), 216 (2011) 525–535. [PubMed: 21384103]

[47]. van Wingerden M, Vinck M, Tijms V, Ferreira IR, Jonker AJ, Pennartz CM, NMDA receptors control cue-outcome selectivity and plasticity of orbitofrontal firing patterns during associative stimulus-reward learning, Neuron, 76 (2012) 813–825. [PubMed: 23177965]

[48]. Thorpe SJ, Rolls ET, Maddison S, The orbitofrontal cortex: neuronal activity in the behaving monkey, Exp Brain Res, 49 (1983) 93–115. [PubMed: 6861938]

[49]. Cai X, Padoa-Schioppa C, Contributions of orbitofrontal and lateral prefrontal cortices to economic choice and the good-to-action transformation, Neuron, 81 (2014) 1140–1151. [PubMed: 24529981]

[50]. Moorman DE, Aston-Jones G, Orbitofrontal cortical neurons encode expectation-driven initiation of reward-seeking, J Neurosci, 34 (2014) 10234–10246. [PubMed: 25080585]

[51]. Sul JH, Kim H, Huh N, Lee D, Jung MW, Distinct roles of rodent orbitofrontal and medial prefrontal cortex in decision making, Neuron, 66 (2010) 449–460. [PubMed: 20471357]

[52]. Young JJ, Shapiro ML, Double Dissociation and Hierarchical Organization of Strategy Switches and Reversals in the Rat PFC, Behavioral Neuroscience, 123 (2009) 1028–1035. [PubMed: 19824768]

[53]. Marquardt K, Sigdel R, Brigman JL, Touch-screen visual reversal learning is mediated by value encoding and signal propagation in the orbitofrontal cortex, Neurobiol Learn Mem, DOI 10.1016/j.nlm.2017.01.006(2017).

[54]. van Wingerden M, Vinck M, Lankelma J, Pennartz CM, Theta-band phase locking of orbitofrontal neurons during reward expectancy, J Neurosci, 30 (2010) 7078–7087. [PubMed: 20484650]

[55]. Tiesinga PH, Sejnowski TJ, Mechanisms for Phase Shifting in Cortical Networks and their Role in Communication through Coherence, Front Hum Neurosci, 4 (2010) 196. [PubMed: 21103013]

[56]. Calderone DJ, Lakatos P, Butler PD, Castellanos FX, Entrainment of neural oscillations as a modifiable substrate of attention, Trends Cogn Sci, 18 (2014) 300–309. [PubMed: 24630166]

[57]. Haider B, Schulz DP, Hausser M, Carandini M, Millisecond Coupling of Local Field Potentials to Synaptic Currents in the Awake Visual Cortex, Neuron, 90 (2016) 35–42. [PubMed: 27021173]

[58]. Lepage KQ, Kramer MA, Eden UT, The dependence of spike field coherence on expected intensity, Neural Comput, 23 (2011) 2209–2241. [PubMed: 21671792]

[59]. Cull-Candy S, Brickley S, Farrant M, NMDA receptor subunits: diversity, development and disease, Curr Opin Neurobiol, 11 (2001) 327–335. [PubMed: 11399431]

[60]. Yashiro K, Philpot BD, Regulation of NMDA receptor subunit expression and its implications for LTD, LTP, and metaplasticity, Neuropharmacology, 55 (2008) 1081–1094. [PubMed: 18755202]

[61]. Cercato MC, Vazquez CA, Kornisiuk E, Aguirre AI, Colettis N, Snitcofsky M, Jerusalinsky DA, Baez MV, GluN1 and GluN2A NMDA Receptor Subunits Increase in the Hippocampus during Memory Consolidation in the Rat, Front Behav Neurosci, 10 (2016) 242. [PubMed: 28133447]

[62]. Quinlan EM, Lebel D, Brosh I, Barkai E, A molecular mechanism for stabilization of learning-induced synaptic modifications, Neuron, 41 (2004) 185–192. [PubMed: 14741100]

[63]. Holehonnur R, Phensy AJ, Kim LJ, Milivojevic M, Vuong D, Daison DK, Alex S, Tiner M, Jones LE, Kroener S, Ploski JE, Increasing the GluN2A/GluN2B Ratio in Neurons of the Mouse Basal and Lateral Amygdala Inhibits the Modification of an Existing Fear Memory Trace, J Neurosci, 36 (2016) 9490–9504. [PubMed: 27605622]

[64]. Hoover WB, Vertes RP, Projections of the medial orbital and ventral orbital cortex in the rat, J Comp Neurol, 519 (2011) 3766–3801. [PubMed: 21800317]

Author Manuscript Author Manuscript Author Manuscript Author Manuscript

[65]. Schilman EA, Uylings HB, Galis-de Graaf Y, Joel D, Groenewegen HJ, The orbital cortex in rats topographically projects to central parts of the caudate-putamen complex, Neurosci Lett, 432 (2008) 40–45. [PubMed: 18248891]

[66]. van der Meer MA, Johnson A, Schmitzer-Torbert NC, Redish AD, Triple dissociation of information processing in dorsal striatum, ventral striatum, and hippocampus on a learned spatial decision task, Neuron, 67 (2010) 25–32. [PubMed: 20624589]

[67]. Corbit LH, Nie H, Janak PH, Habitual alcohol seeking: time course and the contribution of subregions of the dorsal striatum, Biol Psychiatry, 72 (2012) 389–395. [PubMed: 22440617]

[68]. Bergstrom HC, Lipkin AM, Lieberman AG, Pinard CR, Gunduz-Cinar O, Brockway ET, Taylor WW, Nonaka M, Bukalo O, Willis TA, Rubio FJ, Li X, Pickens CL, Winder DG, Holmes A, Dorsolateral striatum engagement interferes with early discrimination learning, Cell Reports, 23 (2018) 1–9. [PubMed: 29617651]

[69]. Buzsaki G, Chrobak JJ, Temporal structure in spatially organized neuronal ensembles: a role for interneuronal networks, Curr Opin Neurobiol, 5 (1995) 504–510. [PubMed: 7488853]

[70]. Buzsaki G, Draguhn A, Neuronal oscillations in cortical networks, Science, 304 (2004) 1926–1929. [PubMed: 15218136]

Author Manuscript Author Manuscript Author Manuscript Author Manuscript

- Neuronal firing rates are altered by corticohippocampal GluN2B deletion, both in the cortex and dorsal striatum.
- GluN2B deletion disrupts communication between the OFC and dorsal striatum driving the continuation of unrewarded responses.
- Our data demonstrate corticostriatal coordination is necessary for optimal behavioral flexibility.
- These results suggest GluN2B containing NMDARs are a key molecular component in mediating neuronal timing.

Author Manuscript Author Manuscript Author Manuscript Author Manuscript

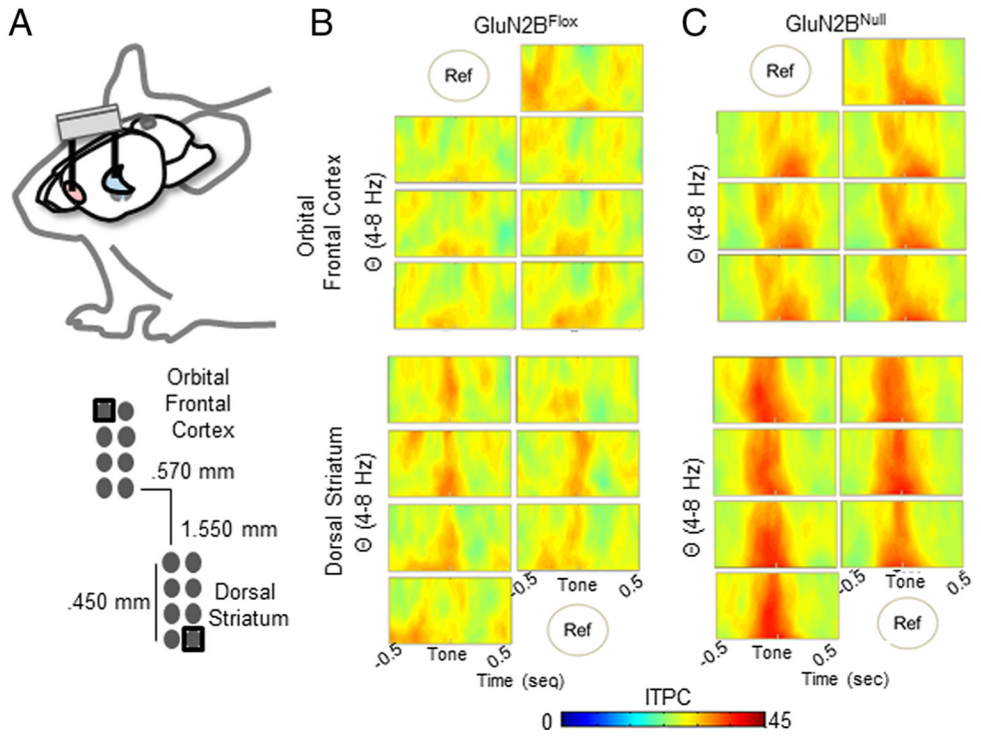

Figure 1. Local LFP Varies Slightly Within Region.

A. Dual implants simultaneously targeted the OFC and dS within each subject. A cerebellar ground screw globally referenced the signals. Additionally, regionally a single electrode was used to control for volume conduction between OFC and dS, which focuses results to local regional activity. **B**. Each electrode within the OFC (top) and DS (bottom) of control mice had a slightly varying, but similar, ITPC Theta (4-8Hz) spectrogram to the cue cessation, indicating little variance in LFP signal over the 0.45mm span of the region the electrode covers. **C.** Similarly, while each electrode within GluN2B^{Null} mice varied slightly within region (OFC top, dS bottom), ITPC within the span of the region had little variance.

Author Manuscript Author Manuscript Author Manuscript Author Manuscript

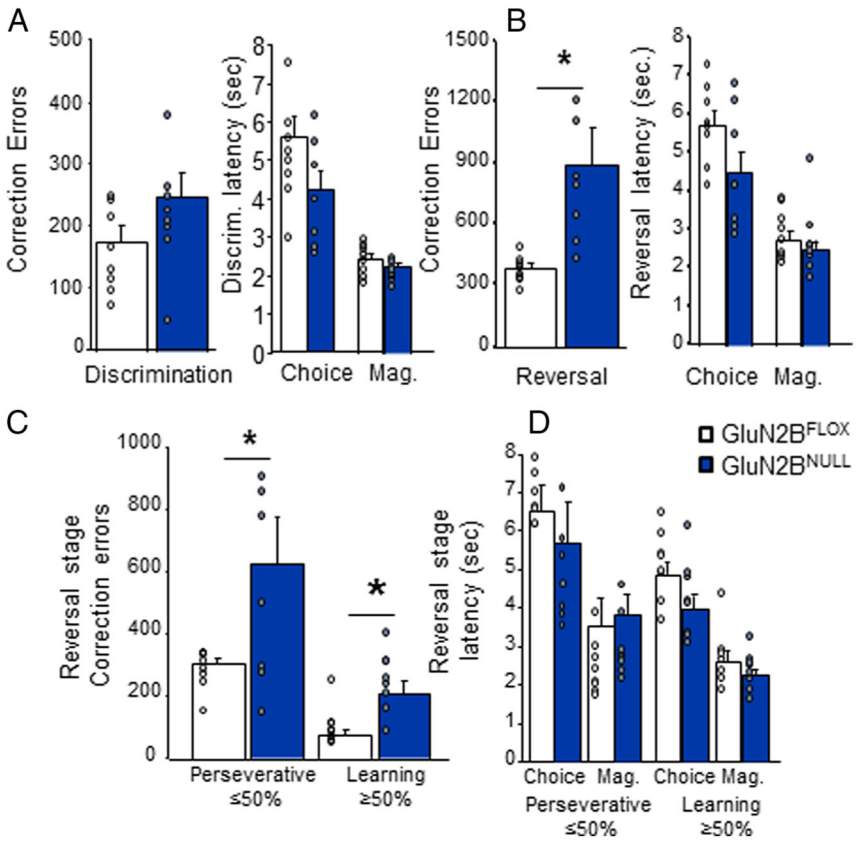

Figure 2: Significantly impaired reversal learning in GluN2B^{NULL} mice.

A. GluN2B^{NULL} mice did not differ from controls on correction errors or response latencies during discrimination. **B**. GluN2B^{NULL} made significantly more correction errors across the reversal problem but did not differ on response latencies. **C**. Correction errors made by GluN2B^{NULL} were significantly higher than control both during the early perseverative and later learning stage of reversal. **D.** No significant differences were seem in response latencies at either stage. N=8 mice per genotype/recording session. * = p<.01

Author Manuscript Author Manuscript Author Manuscript Author Manuscript

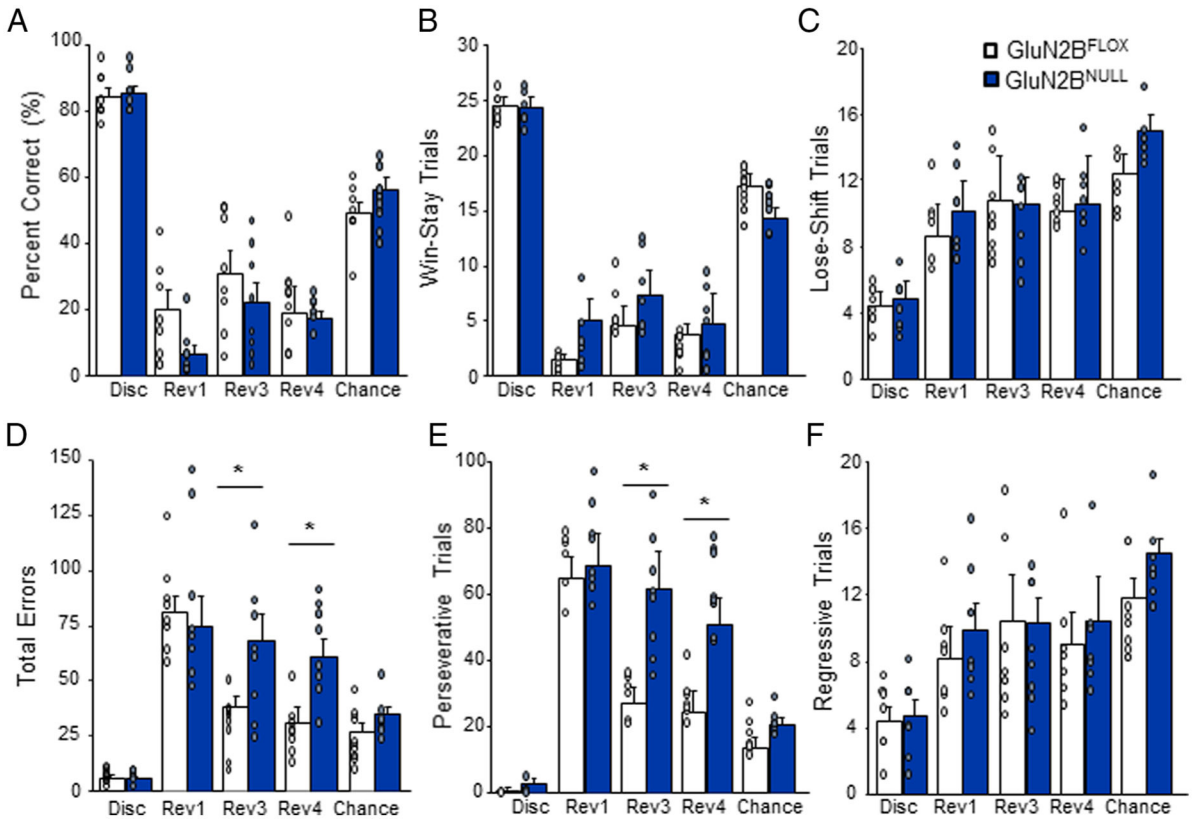

Figure 3: GluN2B^{NULL} mice show increased perseverative responding during early reversal.

A. GluN2B^{NULL} mice did not differ from control on percent correct responding during discrimination or any reversal recording session. **B.** GluN2B^{NULL} mice did not significantly differ from controls on number of *Win-stay* trials made across recording sessions. **C.** *Lose-shift* trials did not significantly differ across genotypes on any recording session. **D.** Total error responding was not different during the first session of reversal but was significantly increased in GluN2B^{NULL}during reversal session 3 and 4. **E.** GluN2B^{NULL} mice made significantly more *Perseverative* error trials during reversal session 3 and 4 compared to controls. **F.** *Regressive* error trials did not significantly differ between genotypes on any session. Data are means ±SEM. N=8 mice per genotype/recording session. * = p<.01

Author Manuscript Author Manuscript Author Manuscript Author Manuscript

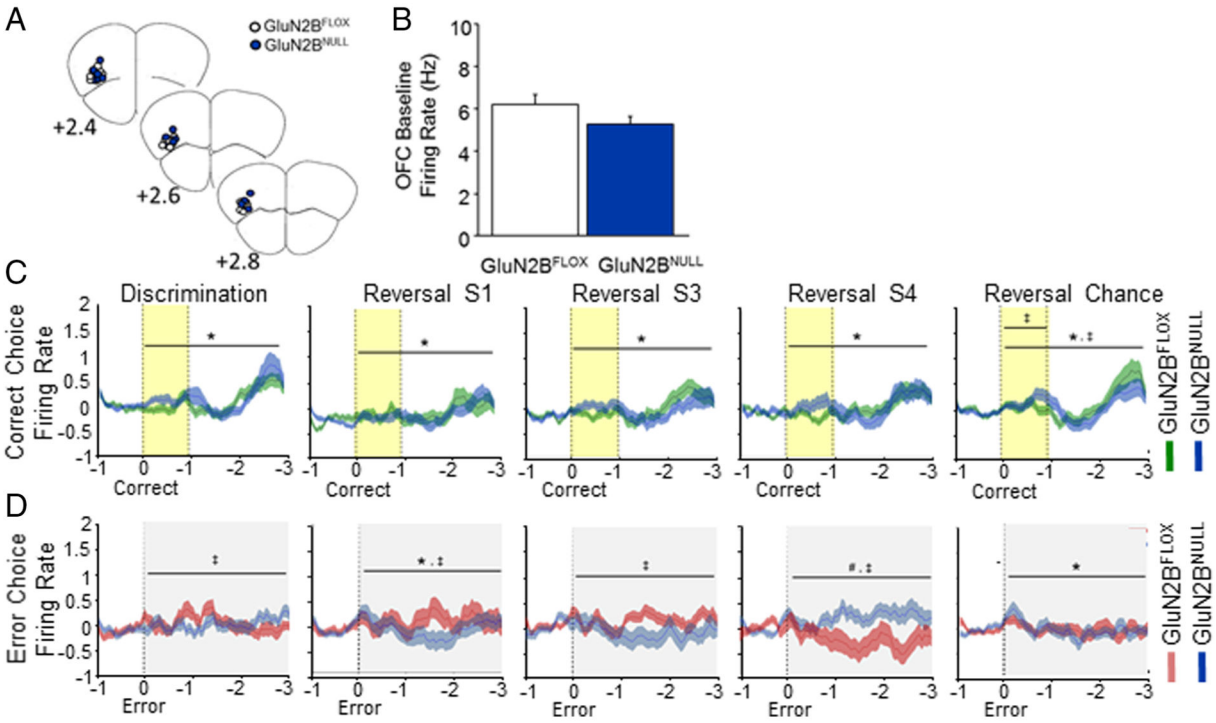

Figure 4: Loss of GluN2B alters OFC firing patterns after error choice.

A. Electrode placement in OFC for GluN2B^{NULL} and GluN2B^{FLOX} controls. **B.** Baseline firing rate of OFC neurons did not differ across genotypes. **C.** OFC neurons increased firing following a correct choice in both genotypes. Firing decreased from discrimination to early reversal before slowly recovering back to discrimination levels. GluN2B^{NULL} had slightly reduced firing immediately following response and during reward approach during chance reversal. **D.** GluN2B^{FLOX} mice showed an increase in firing following an error choice that increased during early reversal sessions 1 and 3. GluN2B^{NULL} mice had significantly decreased error firing during discrimination and reversal session 1 and 3 before significantly increasing during reversal session 4. Firing following an error response significantly increased immediately following the choice during chance reversal but did not differ by genotype. Data are means ±SEM. N=8 mice per genotype/recording session. Yellow band indicates reward cue (tone) and grey band error cue (house light). * = p<.01 main effect of time # = p<.01 main effect of genotype ‡ = p<.01 genotype x time interaction

Author Manuscript Author Manuscript Author Manuscript Author Manuscript

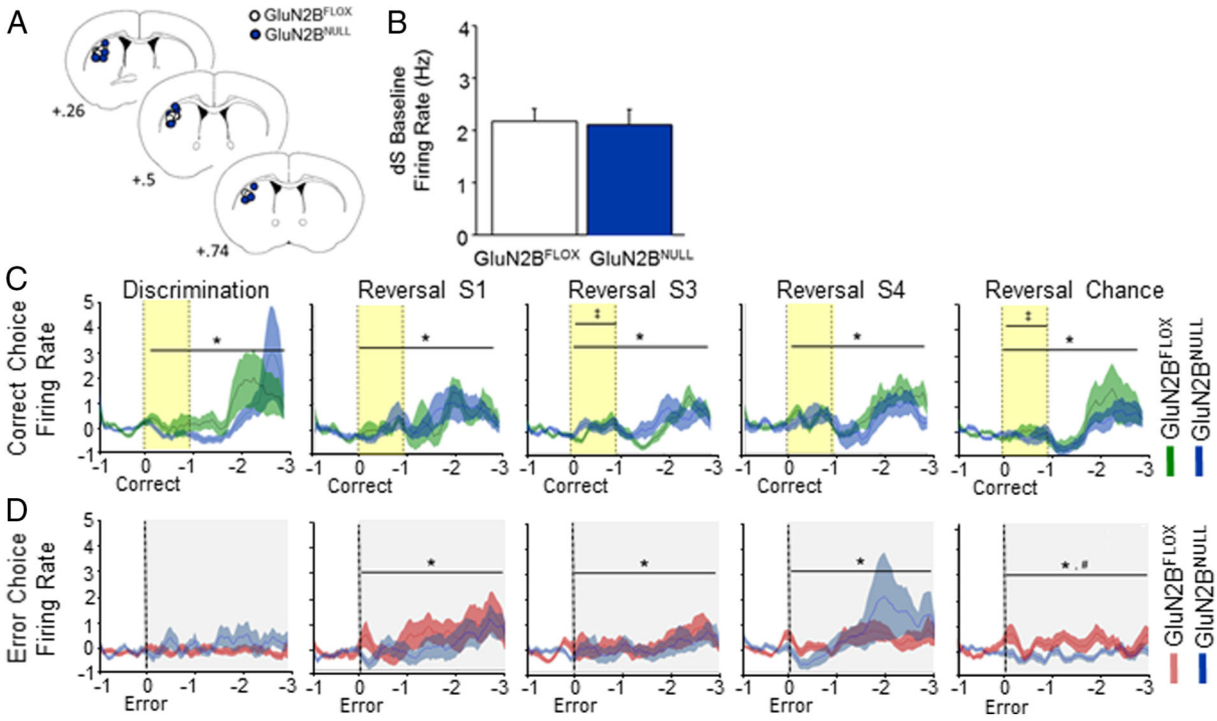

Figure 5: Loss of cortical GluN2B alters dS firing after correct choices.

A. Electrode placement in dS for GluN2B^{NULL} and GluN2B^{FLOX} controls. **B.** Baseline firing rate of dS neurons did not differ across genotypes. **C.** dS neuronal firing increased following a correct choice in both genotypes. Firing decreased from discrimination to early reversal before slowly recovering back to discrimination levels. GluN2B^{NULL} had increased firing immediately following a reward during reversal session 3 and reduced firing during reward approach during chance reversal. **D.** GluN2B^{NULL} and control mice had no change in firing following an error during discrimination. Both genotypes showed significant increases in firing following an error choice during reversal sessions 1, 3 and 4 with no effect of genotype. During chance reversal both groups also showed significant increases in firing following an error, however GluN2B^{NULL} mice had significantly reduced firing versus controls. Data are means ±SEM. N=8 mice per genotype/recording session. Yellow band indicates reward cue (tone) and grey band error cue (house light). * = p<.01 main effect of time # = p<.01 main effect of genotype ‡ = p<.01 genotype x time interaction

Author Manuscript Author Manuscript Author Manuscript Author Manuscript

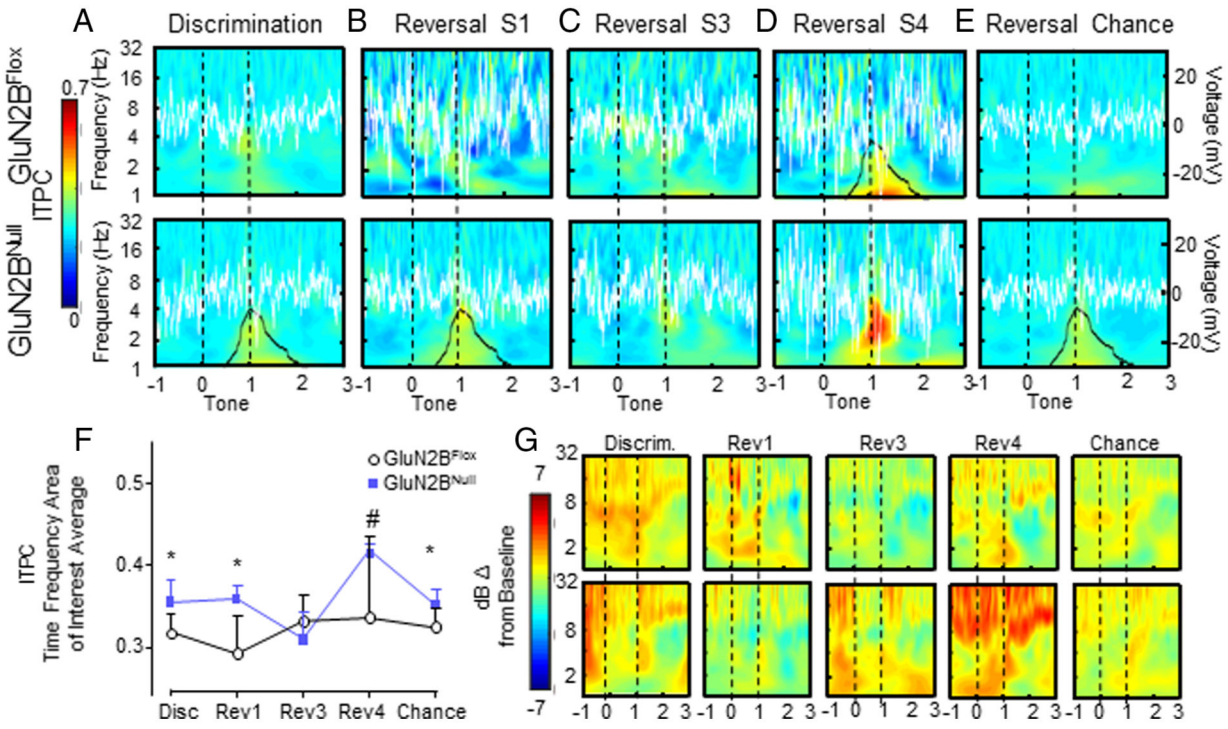

Figure 6: OFC ITPC is increased by loss of corticohippocampal GluN2B.

A. Low levels of OFC ITPC, with a positive ERP in GluN2B^{FLOX} and a negative ERP potential in GluN2B^{NULL}, were seen immediately following the reward cue during discrimination, with significantly higher ITPC response in GluN2B^{NULL}. Delta (1-6Hz) power slightly increased post ITPC response in both genotypes. **B.** ITPC increased in GluN2B^{NULL} versus control during reversal session 1. ERP potential shifts at the reward cue were no longer time locked. **C.** During the third reversal session GluN2B^{NULL} had congruent levels of ITPC and ERP with controls. **D.** ITPC was significantly greater during reversal session 4 than all other sessions in GluN2B^{FLOX} and mutant mice. While and ITPC responses appeared exaggerated in GluN2B^{NULL} during reversal session 4, these changes did not reach significance. Additionally, there were no differences in ERP magnitude response. **E.** ITPC was significantly greater during chance reversal in GluN2B^{NULL} mice compared to controls. No significant differences between genotypes were seen in ERP. **F.** TF-ROI averaged ITPC magnitude average during each session in the OFC. # Main effect of session $p<0.05$, * Significantly different between genotypes $p<0.05$. **G.** dB change from baseline power was not significantly different across sessions or between genotypes. N=8 mice per genotype/recording session. Event related potential voltage is indicated by white line. Overall ITPC is shown via heat map. Black outline denotes significant difference between genotypes in the ROI (bottom row) or significant difference from all other sessions (top row)

Author Manuscript Author Manuscript Author Manuscript Author Manuscript

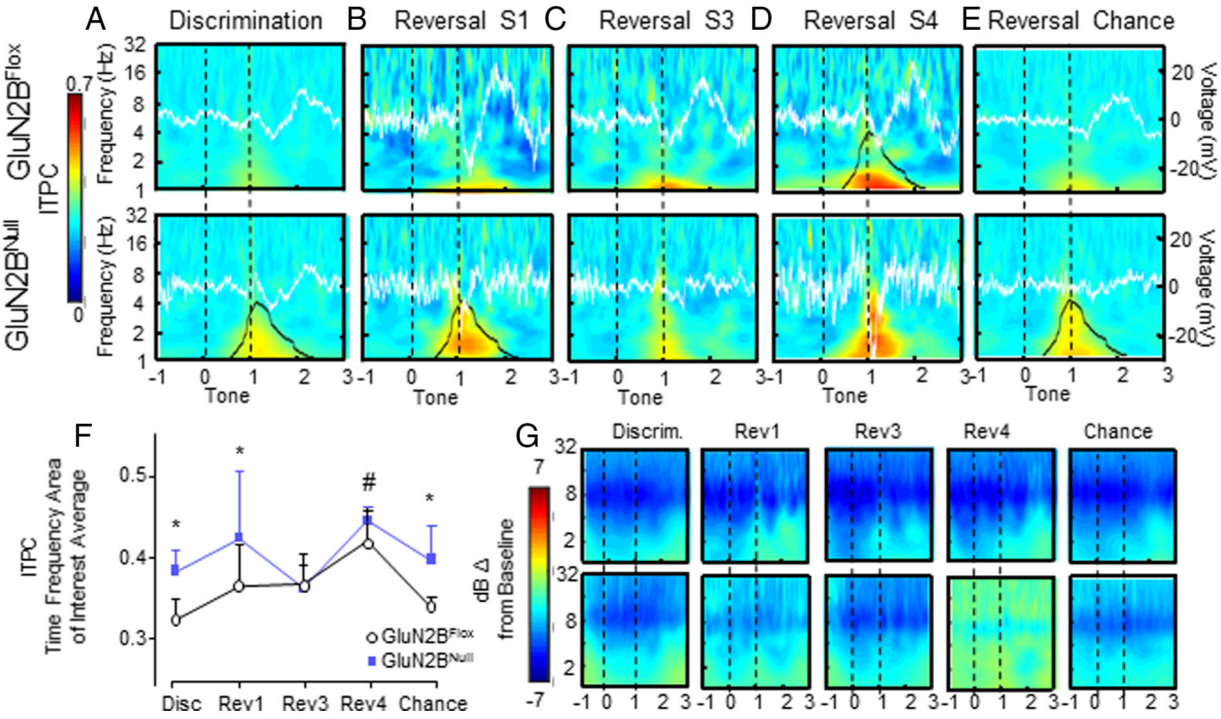

Figure 7: Loss of cortical GluN2B significantly increases dS ITPC.

A. Low levels of dS ITPC were seen across genotypes immediately following the reward cue during discrimination, with a significantly higher response in GluN2B^{NULL} compared to controls. GluN2B^{NULL} and controls displayed a decreased similar potential shift in ERP. GluN2B^{NULL} and controls had a lasting increase in power response after the reward cue, until average reward retrieval. **B.** Upper and lower frequency ITPC remained elevated in GluN2B^{NULL} versus control during reversal session 1. Peak ERP potential shift at time of reward cue was significantly decreased compared to discrimination but was not significantly different between genotypes. **C.** During the third reversal session, GluN2B^{NULL} had equivalent ITPC responses to controls. ERP magnitude was not significantly different between genotypes. **D.** GluN2B^{NULL} had equivalent ITPC response during reversal session 4. ERP potential change at reward cue increased in magnitude, but was not significantly different between genotypes. **E.** GluN2B^{NULL} and GluN2B^{FLOX} mice had significantly increased ITPC once chance criterion had been re-attained. ERP did not significantly differ between genotypes. **F.** TF-ROI averaged ITPC magnitude average during each session. # Significantly different from all sessions $p<0.05$, * Significantly different between genotypes $p<0.05$. **G.** dB change from baseline power was not significantly different across sessions or between genotypes. N=8 mice per genotype/recording session. Event related potential voltage is indicated by white line. Overall ITPC is shown via heat map. Black outline denotes significant difference between genotypes in the TF-ROI (bottom row) or significant difference from all other sessions (top row)

Author Manuscript
Author Manuscript
Author Manuscript
Author Manuscript

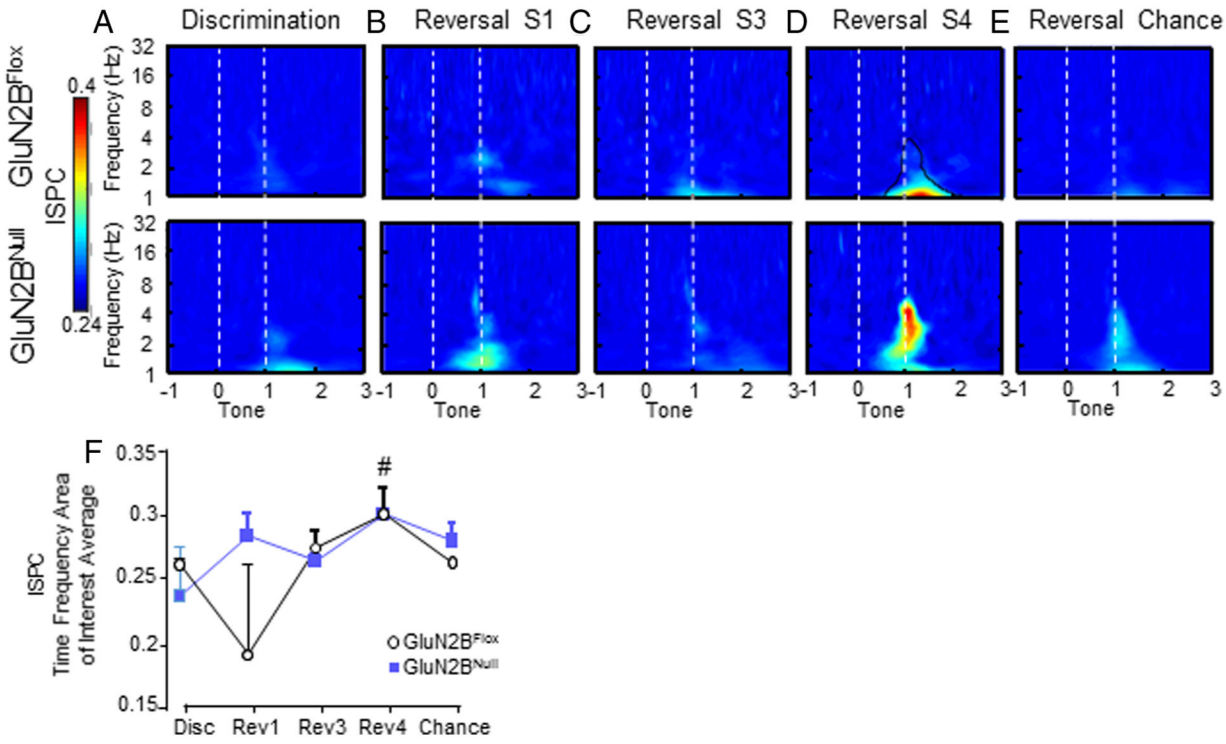

Figure 8: OFC-dS phase functional connectivity is significantly increased in GluN2B^{NULL} mice.

A. Inter-site phase consistency (ISPC) was seen in low levels in the low delta- theta range (1-5 Hz) for GluN2B^{NULL} mice during discrimination. **B.** ISPC increased in both GluN2B^{FLOX} and GluN2B^{NULL} during the first session of reversal compared to discrimination, with higher levels in GluN2B^{NULL} compared to controls. **C.** ISPC continued into reversal session 3, with differences in peak frequency of connectivity, GluN2B^{NULL} being within the low theta range ~4 Hz and GluN2B^{FLOX} in delta range ~1.5 Hz. **D.** During the final reversal session, before chance performance was reached, ISPC was robust in both genotypes, and significantly increased in GluN2B^{NULL} mice, specifically in the theta range of ~4 Hz. **E.** When chance was re-attained during reversal, OFC-dS ISPC returned to discrimination levels in GluN2B^{NULL} mice, but remained elevated in GluN2B^{FLOX} mice. **F.** Average ISPC within the TF-ROI plotted against session. There was a significant main effect of gentoype with GluN2B^{NULL} showing elevated ISPC, but no significant differences in ITPC by session between GluN2B^{NULL} mice and controls. Reversal S4 had significantly greater ISPC compared to all other sessions in controls. # $p < 0.05$ in controls, compared to all other sessions.

Author Manuscript
Author Manuscript
Author Manuscript
Author Manuscript

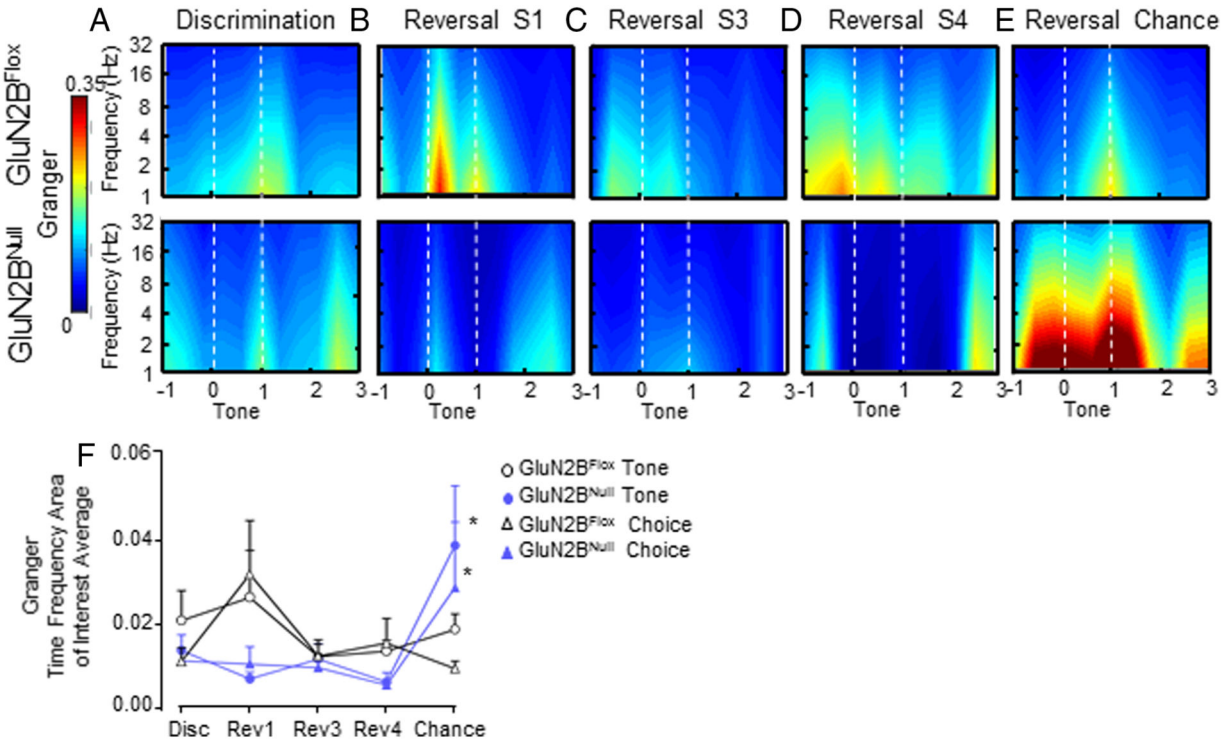

Figure 9: Granger prediction of OFC to dS functional connectivity is significantly increased in GluN2B^{NULL} mice.

A. Low levels of OFC to dS information transfer immediately after reward cue in GluN2B^{FLOX} mice, and additionally before reward retrieval in GluN2B^{NULL} mice. **B.** The majority of OFC to dS connectivity was shifted to immediately after a correct choice during the first session of reversal in GluN2B^{FLOX} mice, and this response was blunted in GluN2B^{NULL} mice, but not significantly. **C.** GluN2B^{FLOX} mice maintain OFC to dS connectivity at time of choice during reversal S3, which again is decreased but not significantly in GluN2B^{NULL} mice. **D.** GluN2B^{FLOX} connectivity remains elevated during reversal chance at time of choice on reversal S4, while GluN2B^{NULL} mice remain to have decreased connectivity. **E.** Once chance criterion is re-attained Granger prediction in GluN2B^{FLOX} mice returns to end of reward cue timing at levels similar to those during initial discrimination. However, GluN2B^{NULL} mice have significantly elevated OFC to dS connectivity on reversal chance. **F.** Average Granger prediction vales within the Choice and Tone TF-ROIs across sessions. Dotted lines (-----) demarcate choice and offset of associative tone. Black rectangles represent significant effect of genotype. * $p<0.05$ between genotypes.